

CIRCULAR, HEXAGONAL AND OCTAGONAL ARRAY GEOMETRIES FOR SMART ANTENNA SYSTEMS USING HYBRID CFO-HC ALGORITHM

**A. M. Montaser, K. R. Mahmoud, Adel B. Abdel-Rahman,
H. A. Elmikati Senior Member IEEE**

¹Sohag University, Sohag, Egypt.

²Helwan University, Helwan, Egypt.

³South Valley University, Qena, Egypt.

⁴Mansoura University, Mansoura 35516, Egypt.

(Received February 23, 2012 Accepted September 1, 2012)

ABSTRACT:

In this paper, circular, hexagonal and Octagonal array geometries for smart antenna applications are compared. Uniform circular (UCA), uniform hexagonal (UHA) and uniform Octagonal arrays (UOA) with 24 half-wave dipole elements are examined. An efficient global hybrid optimization method is proposed combining the Central Force Optimization (CFO) as a global optimizer and Hillclimbing (HC) algorithm as a local optimizer. After the final global iteration, a local optimization can be followed to further improve the solution obtained from the CFO. The CFO-HC algorithm is used to optimize the complex excitations, amplitudes and phases, of the adaptive arrays elements for beamforming, the CFO-HC algorithm was implemented using MATLAB-software and linked to the CST simulator to simulate the adaptive arrays.

Index Terms- Uniform circular arrays (UCA), Uniform hexagonal arrays (UHA), Uniform octagonal arrays (UOA), Hybrid CFO-HC algorithm.

1. INTRODUCTION

Smart antennas refer to a group of antenna technologies that increase communication systems capacity by reducing the co-channel interference and increase the quality by reducing the fading effects [1]. A smart antenna array containing M identical elements can steer a directional beam to maximize signals of interest (SOI), while nullifying the signals from other directions, signals not of interest (SNOI) [2]. The array geometries that have been studied include mainly uniform linear arrays (ULA), uniform rectangular (URA), and uniform circular arrays (UCA). A ULA has excellent directivity and it can form the narrowest main-lobe in a given direction, but it does not work equally well in all azimuthal directions. A major disadvantage of the URA is that an additional major lobe of the same intensity appears on the opposite side. An obvious advantage results from the symmetry of the circular array structure. Since a circular array does not have edge elements, directional patterns synthesized with a circular array can be electronically rotated in the plane of the array without a significant change of the beam shape [3]. Concerning the two geometries, the URA and the planar uniform circular array (PUCA) with similar areas, slightly greater directivity was

obtained with the use of the PUCA [4]. A circular array produces radiation pattern high side-lobe geometry. If the distance between the array elements is decreased to reduce the sidelobes, the mutual coupling influence becomes more significant. For mitigating high side-lobe levels multi-ring arrays are utilized. Furthermore, a hexagonal array is presented for smart antenna applications to overcome the problem of high side-lobes [5]. A structure consisting of six circular patches non-uniformly distributed along the perimeter of an antenna array and one antenna in the center has been previously examined and compared with a circular structure [6]. It was found that it was possible to configure the array to obtain directional patterns with high gain and directivity for circular and hexagonal arrays. Also, best steerability was obtained using a uniform array of seven patch antennas, configured as a hexagon with a central element [6].

The techniques of placing nulls in the antenna patterns to suppress interference and maximizing their gain in the desired direction have received considerable attention in the past and are still of great interest using evolutionary algorithms such as genetic algorithms (GA) [7,8] or the sequential quadratic programming (SQP) algorithm [2]. It is recognized that the Particle Swarm Optimization PSO algorithm is a practical and powerful optimization tool for a variety of electromagnetic and antenna design problems [9–14]. Compared with other evolutionary algorithms such as the GA and simulated annealing (SA), the PSO algorithm is much easier to understand and implement and requires minimum mathematical processing. In recent years, various versions of the PSO algorithm have been successfully used in linear [15, 16] and circular antenna array synthesis problems [17, 18].

Many of the attempts on antenna array synthesis assume that the elements of the array are represented by isotropic point sensors isolated from each other or the element pattern may be modeled by a cosine function. However, in practice, the elements of antenna arrays have finite physical dimensions and specific radiation characteristics. Since most of the beamforming algorithms ignore the effects of mutual coupling, the predicted system performances may not be accurate, especially in closely spaced antenna elements. Therefore, to evaluate accurately the resulting system performance of practical antenna arrays, the electromagnetic influence among the elements must be carefully considered. More recently, much attention has been paid to the effects of mutual coupling [19–22].

The methods of beam pattern synthesis generally based on controlling the complex weights (the amplitude and phase), the excitation amplitude only, the phase only, and the element position only have been extensively considered in the literature [2, 7, 14, 23]. The most important method is based on controlling the complex weights. This technique fully exploits the degrees of freedom for the solution space. Furthermore, the sidelobe level (SLL) and the main beam characteristics can be controlled. On the other hand, it is also the most expensive technique considering the cost of both a phase shifter and a variable attenuator for each array element. Furthermore, when the number of elements in the antenna array increases, the computational time to find the values of element amplitudes and phases will also increase. There are a trade-off between the quality of the constrained pattern and the complexity of the electronic control. The antenna system is analyzed completely using option in program Computer Simulation Technology (CST Microwave Studio) software, which is linked to the CFO-HC

algorithm programmed using MATLAB-software to optimize the antenna system parameters. Interchanging information between CST Microwave studio and Matlab allows the implementation optimization algorithms are not included in the Microwave studio environment itself.

In this paper, the CFO-HC is used to optimize the weights of phase shift and amplitude of the excitation of each element of the array for beamforming synthesis. The CFO-HC algorithm program was implemented using MATLAB-software and linked to CST Microwave Studio to simulate the antenna arrays. A comparative study of several different array geometries using 24 half-wave dipole elements in free space is also included.

2. A hybrid CFO-HC Algorithm

Generally, the hybrid method combining two algorithms is considered for the global optimization of multi-optimum functions. To localize a “promising area”, likely to contain a global optimum, it is necessary to well “explore” the whole search domain. When a promising area is detected, the appropriate tools must be used to “exploit” this area and obtain the optimum as accurately and quickly as possible. Both tasks are hardly performed through only one method. Therefore, the global metaheuristic CFO is used to localize the “best” areas and Hillclimbing as a local search method to refine the results [24].

The CFO algorithm finds the optima of an objective function $f(x_1, \dots, x_{N_d})$ by flying a set of probes through the decision space (DS) along trajectories computed using the gravitational analogy. In an N_d -dimensional real valued decision space, each probe p with position vector $\vec{R}_{j-1}^p \in \mathbb{R}^{N_d}$ experiences acceleration \vec{A}_{j-1}^p at the discrete time step $(j - 1)$ given by:

$$\vec{A}_{j-1}^p = G \sum_{\substack{k=1 \\ k \neq p}}^{N_p} U \left(M_{j-1}^k - M_{j-1}^p \right) \left(M_{j-1}^k - M_{j-1}^p \right)^\alpha \frac{\left(\vec{R}_{j-1}^k - \vec{R}_{j-1}^p \right)}{\left\| \vec{R}_{j-1}^k - \vec{R}_{j-1}^p \right\|^\beta} \quad (1)$$

where N_p is the total number of probes; $p = 1, \dots, N_p$ is the probe number; $j = 0, \dots, N_t$ is the time step; G is the gravitational constant; \vec{R}_{j-1}^p is the position vector of probe p at step $j - 1$; $M_{j-1}^p = f \left(\vec{R}_{j-1}^p \right)$ is the fitness value at probe p at time step $j - 1$; $U()$ is the Unit Step function; and β, α are the CFO exponents [25-28].

CFO mass is defined as the difference of fitnesses raised to the power α multiplied by the Unit Step function. It should be emphasized that CFO mass is not the value of the objective function itself. The Unit Step $U()$ is essential because it creates positive mass, thus insuring that CFO’s gravity is attractive. Each probe’s position vector at step j is updated according to the following equation:

$$\vec{R}_j^p = \vec{R}_{j-1}^p + \frac{1}{2} \vec{A}_{j-1}^p \Delta t^2; j \geq 1 \quad (2)$$

Δt is the time step increment (unity in this paper). CFO starts with a user-specified initial probes positions and accelerations distributions. The initial acceleration vectors are usually set to zero.

However, the probes may fly outside the decision space and in this case it should be

returned or replaced with other probes inside DS. There are many possible probe retrieval methods. A useful one is the reposition factor F_{rep} , which plays an important role in CFO's convergence [26].

If the probe $\vec{R}_j^p(i)$ falls below R_i^{min} then it is assigned to be:

$$\vec{R}_j^p(i) = R_i^{\text{min}} + F_{\text{rep}} \left[\vec{R}_{j-1}^p(i) - R_i^{\text{min}} \right] \quad (3)$$

But, if the probe $\vec{R}_j^p(i)$ is greater than R_i^{max} then:

$$\vec{R}_j^p(i) = R_i^{\text{max}} - F_{\text{rep}} \left[R_i^{\text{max}} - \vec{R}_{j-1}^p(i) \right] \quad (4)$$

where, R_i^{min} and R_i^{max} are the minimum and maximum values of the i th spatial dimension corresponding to the optimization problem constraints. In general, the range of F_{rep} is set from 0 to 1, or it may be variable [28]. In this paper the reposition factor is set to be 0.05 according the number of iteration. After every k^{th} step the DS size is adaptively reduced around the probe's location with the best fitness, R_{best} where the DS's boundary coordinates will be reduced by one-half coordinate-by-coordinate basis [29]. Thus,

$$\hat{R}_i^{\text{min}} = R_i^{\text{min}} + \frac{1}{2} (R_{\text{best}} - R_i^{\text{min}}) \quad (5)$$

$$\hat{R}_i^{\text{max}} = R_i^{\text{max}} - \frac{1}{2} (R_i^{\text{max}} - R_{\text{best}}) \quad (6)$$

The obtained probes position will be considered to calculate the new fitnesses and the accelerations. These steps will be repeated till the last time step N_t . Now the global optima using CFO deterministic algorithm is completed; the Hillclimbing (HC) local optimization technique is followed to fine optimize the results. The HC method thus falls in the general class of direct search methods. It is an iterative algorithm that starts with an arbitrary solution to a problem, then attempts to find a better solution by incrementally changing a single element of the solution. If the change produces a better solution, an incremental change is made to the new solution. Then repeating the steps until no further improvements can be found [30], Figure 1 shows flowchart for the main steps of the hybrid CFO-HC algorithm.

The CFO-HC algorithm programmed using MATLAB is interfaced with the standard software CST Microwave Studio to accomplish the antenna designs. Using MATLAB to control the CST Microwave Studio solver creates a powerful tool for design, analysis, and control. The antenna is analyzed completely using CST Microwave Studio, then the CST program is linked with the CFO-HC algorithm using MATLAB-program to optimize the antenna. Interchanging information between CST Microwave studio and Matlab allows the implementation of mathematical or optimization algorithms and graphical possibilities which are not included in the Microwave studio environment itself. The approach developed here is very flexible and utilizes the inherent capability of Microwave studio to execute Visual Basic for Applications (VBA) programs. The general idea of this method is that Matlab and

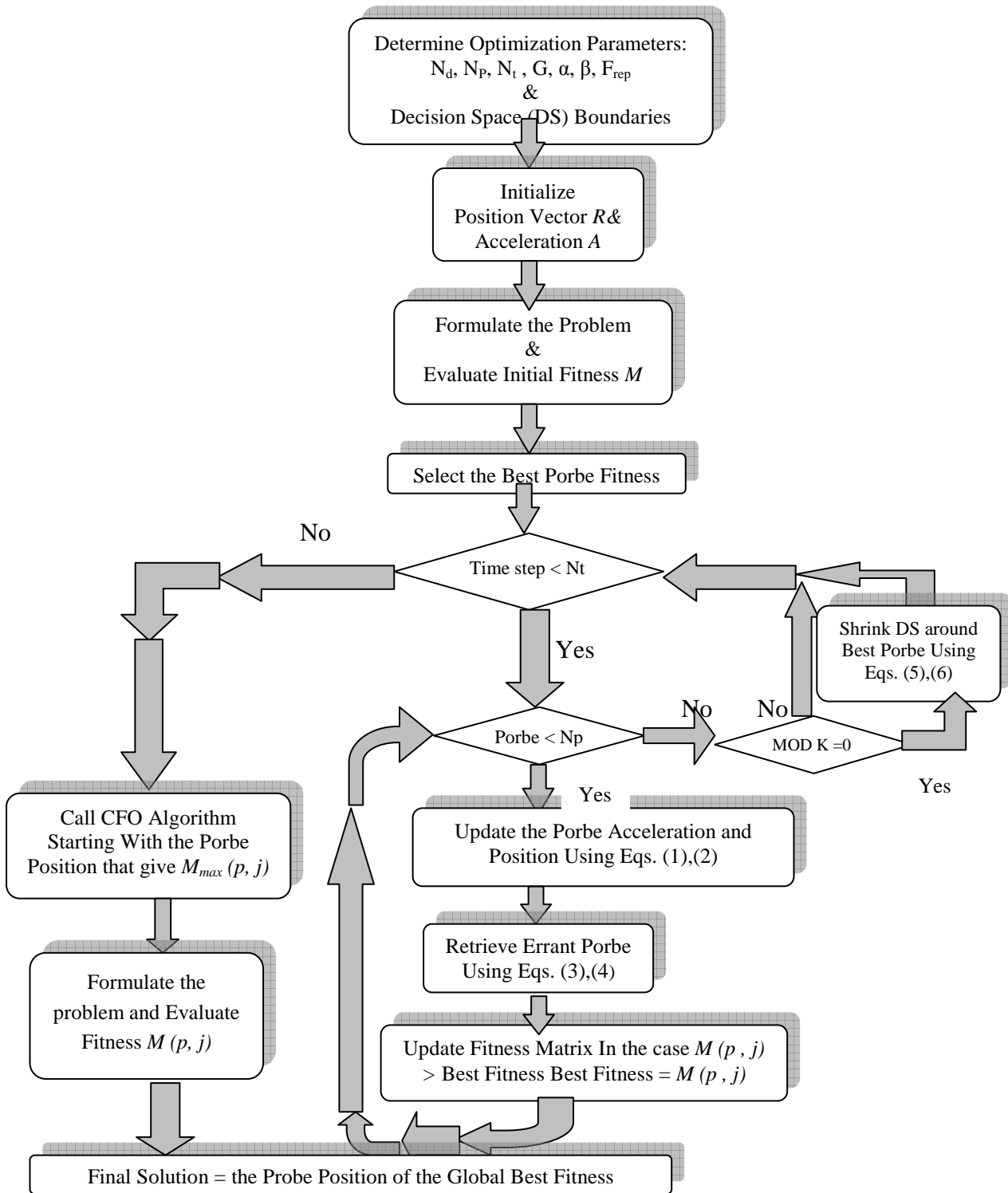


Figure 1. Flowchart showing the main steps of the hybrid CFO-HC algorithm

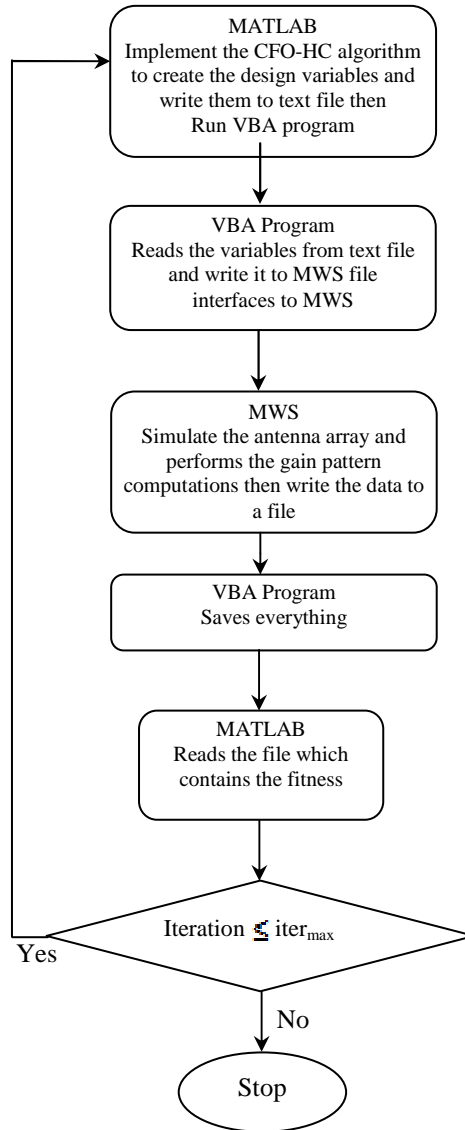


Figure 2. Flowchart showing the main steps to link the MATLAB with the CST simulator.

Microwave studio can interchange information using external text files, which can be read and written by both programs [31]. Figure 2 shown flowchart for the main steps to link the MATLAB with the CST simulator.

3. OBJECTIVE FUNCTION

The objective function provides the interface between the physical problem

and the optimization algorithm. In general this could be the antenna gain, directivity, SLL, peak cross-polarization, and weight, or some kind of weighted sum of all these factors. So the quality of an antenna beamforming is expressed mathematically by an objective function. The following objective function rewards the antenna array for maximizing the output power toward the desired signal at φ_i and minimizing the total output power in the direction of the interfering signals at φ_j .

$$\text{Objective function} = \sum_{i=1}^N a_i G(\varphi_i) - \sum_{j=1}^M b_j G(\varphi_j)$$

where G is the antenna array gain and the constants a_i and b_j are the weights that control the contribution from each term to the overall objective function. The constant N represents the number of desired users, and M represents the number of interferers. In our analysis, we take $N = 1$ and $M = 2$. The weights a_i and b_j are considered to be $(a_1 = 20)$, $(b_1 = 1)$, and $(b_2 = 1)$ to give a higher priority to maximizing the output power toward the desired signal while minimizing the total output power in the direction of the interfering signals.

4. ARRAY GEOMETRIES

The circular, hexagonal and octagonal arrays using half-wave dipole elements are presented and compared with each other. The first considered array is a UCA, the geometry of the array is shown in Figure 3a. The geometry consists of 24 elements uniformly distributed with a ring of a radius $r = (12/2\pi) \lambda$. The second array is a UHA of hexagonal geometry consists of 24 elements array with a radius $r = (12/2\pi) \lambda$ as shown in Figure 3b. The third type of arrays is a UOA, it consists of 24 elements array with a radius $r = (12/2\pi) \lambda$ as shown in Figure 3c. The antenna elements in all cases consist of vertical (z - directed) half-wave dipole elements equally spaced in the x - y plane along a closed ring, where the distance between adjacent elements is $d_c = 0.5 \lambda$ and the dipole wire radius is $a = 0.003369 \lambda$.

4.1. EQUALLY AMPLITUDE AND PHASE EXCITATION

To illustrate the difference between circular, hexagonal and octagonal arrays geometries, the normalized radiation pattern for each case is plotted first, assuming all elements are excited with the same amplitude equal 1 and phase equal 0. Figure 4 shows the normalized radiation pattern for the UCA. Figure 5 presents the normalized radiation pattern for the UHA and Figure 6 illustrates the normalized radiation pattern for the UOA. It can be observed from these plots that, the circular arrangement can give better steerability and higher gain characteristics than the hexagonal and octagonal arrangements for uniform arrays.

4.2. BEAMFORMING OF SMART ANTENNA ARRAYS

Now, as an example of adaptive beamforming with all arrays geometries, we considered the desired user at $\phi = 180^\circ$ while the other two users are at $\phi = 60^\circ$ and $\phi = 270^\circ$, which are considered as interferers. Figure 7, 8, 9 shows the resulting normalized gain pattern for the UCA, UHA, and UOA respectively using half-wave dipole elements. A comparison between

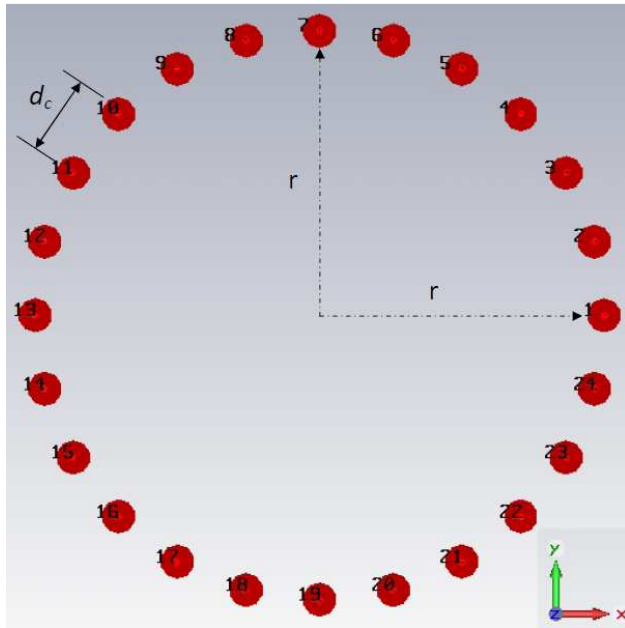


Figure 3a. Circular array geometries

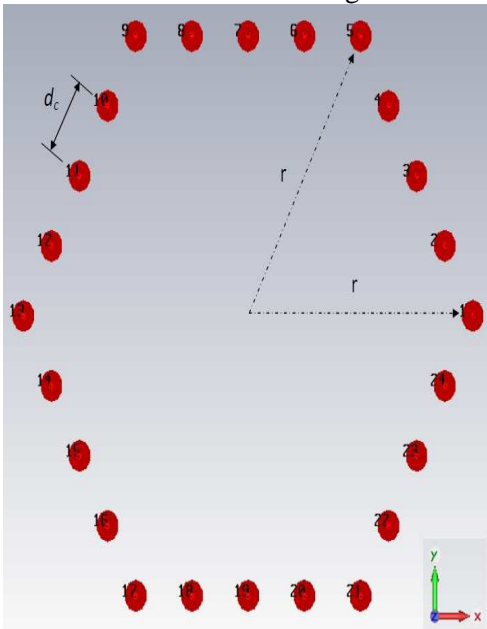


Figure 3b. Hexagonal array geometries

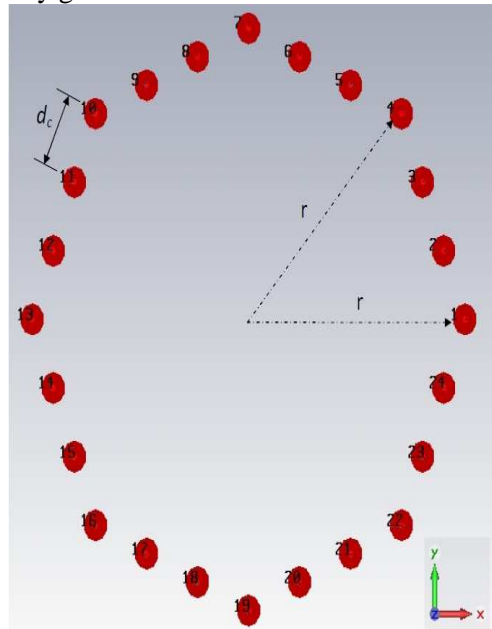
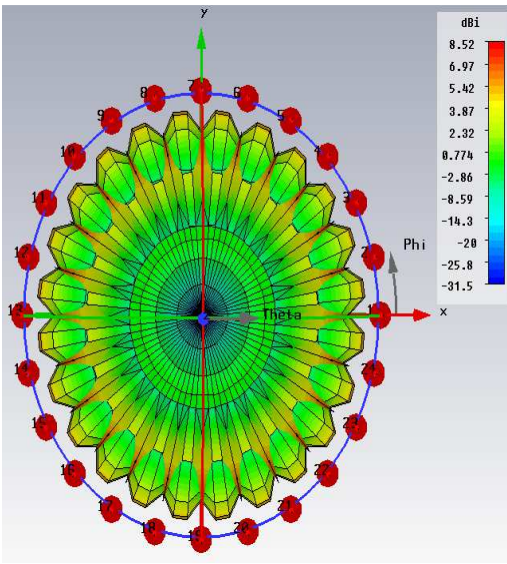
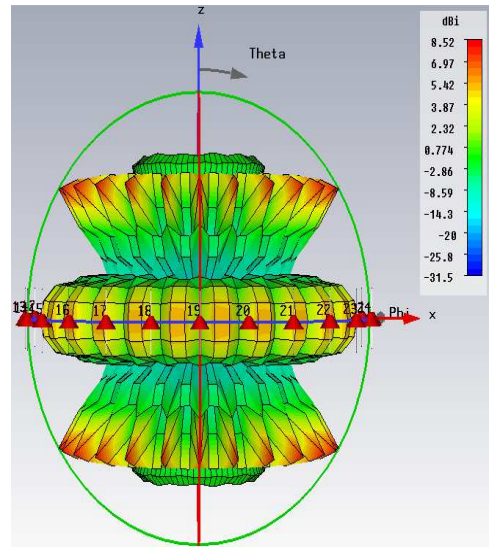


Figure 3c. Octagonal array geometries

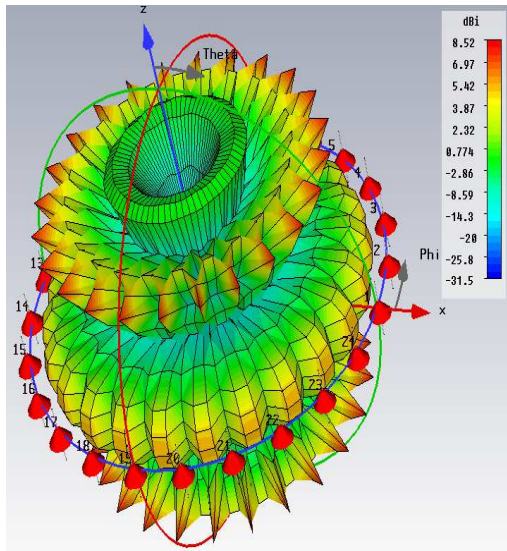
Figure 3. The array geometries



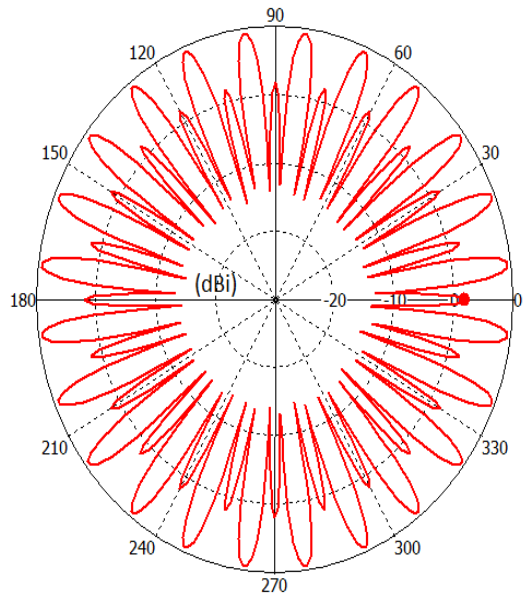
(a) Top View



(b) side view

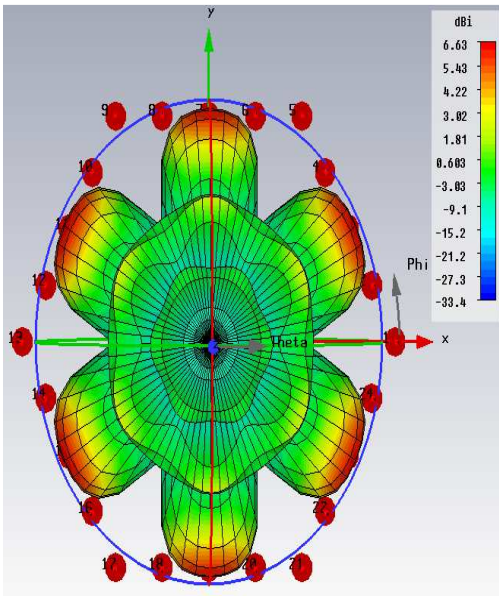


(c) 3-D

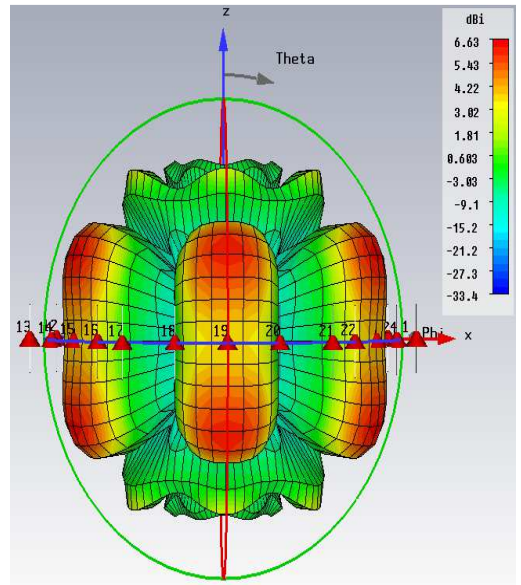


(d) Polar plot at xy-Plane

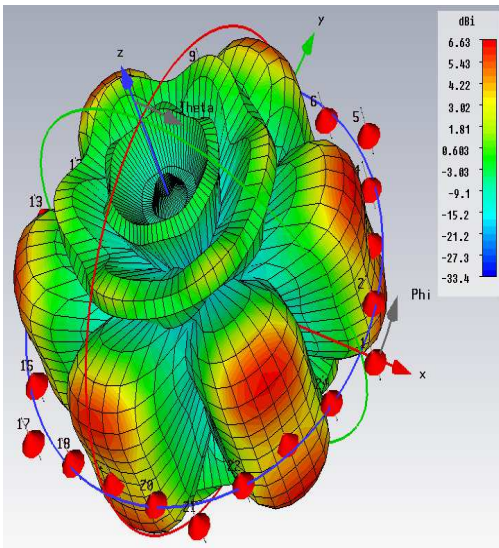
Figure 4. Normalized radiation pattern for the circular array



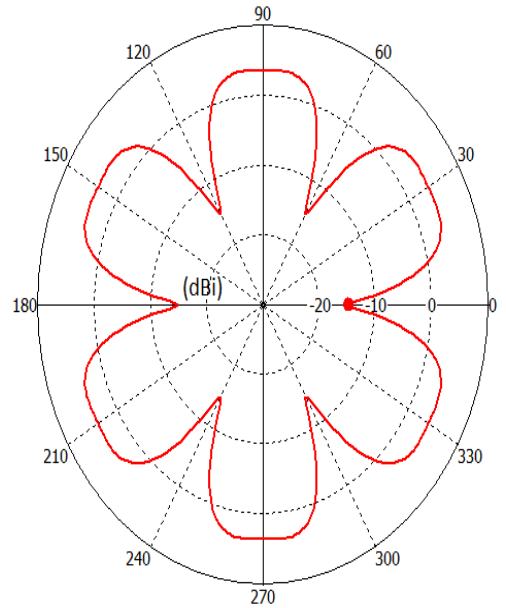
(a) Top View



(b) side view

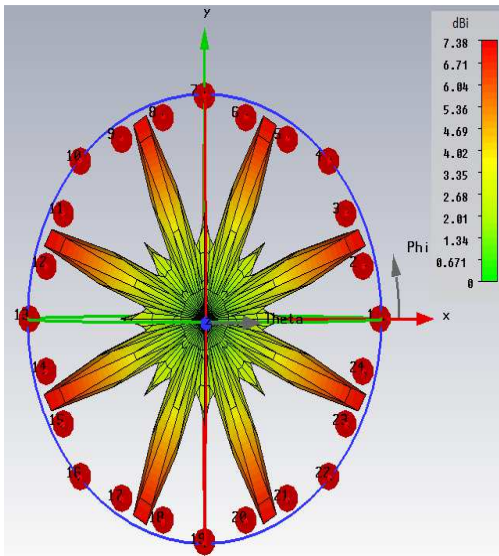


(c) 3-D

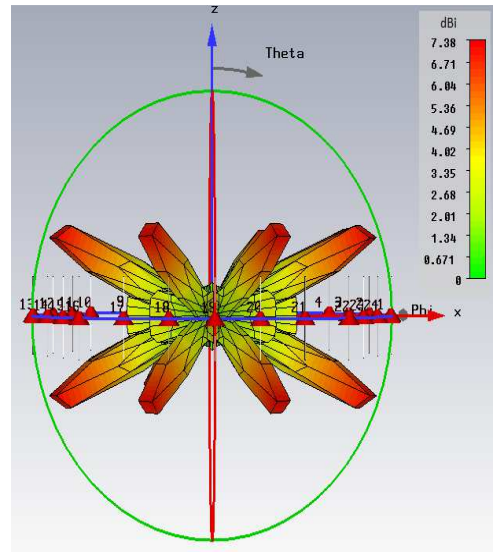


(d) Polar plot at xy-Plane

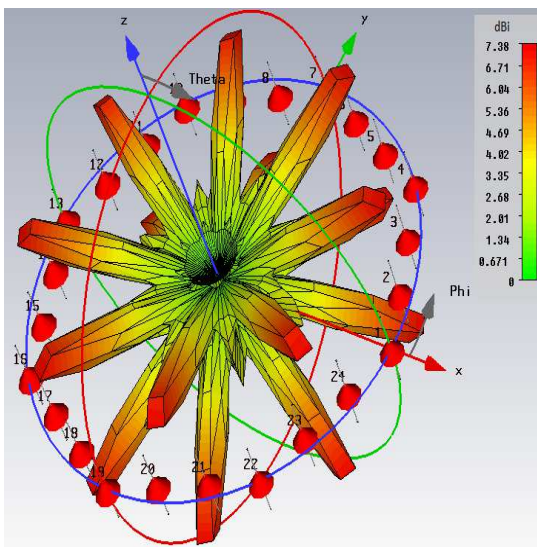
Figure 5. Normalized radiation pattern for the hexagonal array



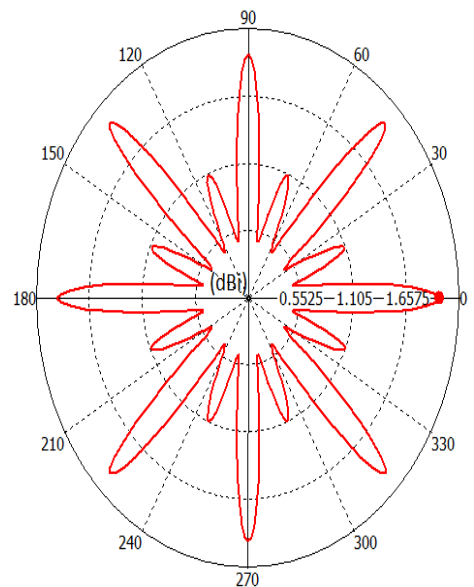
(a) Top View



(b) side view



(c) 3-D



(d) Polar plot at xy-Plane

Figure 6. Normalized radiation pattern for the octagonal array

the resulting normalized gain pattern for the UCA, UHA and UOA using half-wave dipole elements is presented in Figure 10.

The CFO-HC algorithm shows good performance in directing the maximum gain towards the direction of the SOI while placing deep nulls towards the angles of SNOIs even when the mutual coupling between elements is fully taken into account. The CFO-HC algorithm with 20 probe size and 50 time steps. It required about 13 minutes on a desktop (Dual Core Intel (tm) Processor of 3.2 GHz) to get the result. This time can be reduced very significantly by calculating the Z-matrix of the antenna array,

which takes most of the time, only once and calling it when needed instead of calculating it each time ($100 * 200$). For example, the time required is only 24 sec when the same array is implemented using isotropic elements (where the Z-matrix calculation is not required). Also, it is not necessary to wait until the end of all iterations; the program can be ended when acceptable results are obtained. For beamforming synthesis, the amplitude was allowed to vary between 1.0 and 3.0 and the phase is allowed to vary between $-\pi$ and π .

The required amplitude and phase excitations of each element to obtain the beam patterns in Figures 7, 8 and 9 as well as the directivity comparison between the different types of array are shown in Table 1. It is noted that, the hexagonal array geometries achieves slightly deeper nulls towards the angles of interfering signals with an increase in gain around 1.86 dB compared with the circular array geometries and increase in gain around 0.75 dB compared with the octagonal array geometries. Also, as a comparison between circular, hexagonal and octagonal array geometries, it is noted that the area of the circular array is $(3.14r^2)$ but for hexagonal array geometry the area is $(2.16r^2)$, while the octagonal array geometry the area is $(2.83r^2)$, thus the area hexagonal array is less than those circular array and octagonal array.

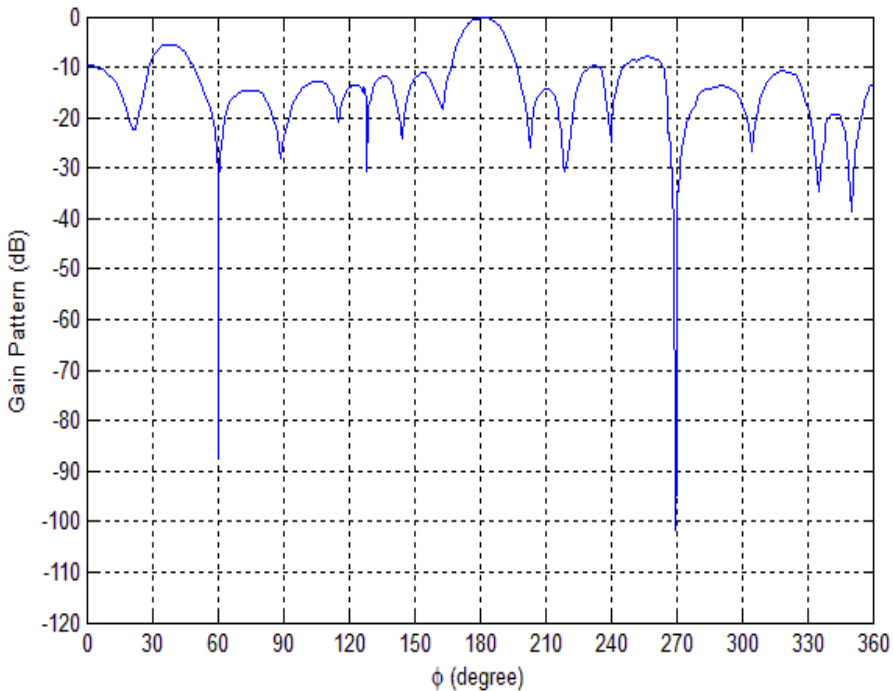


Figure 7. Normalized gain pattern for the circular array

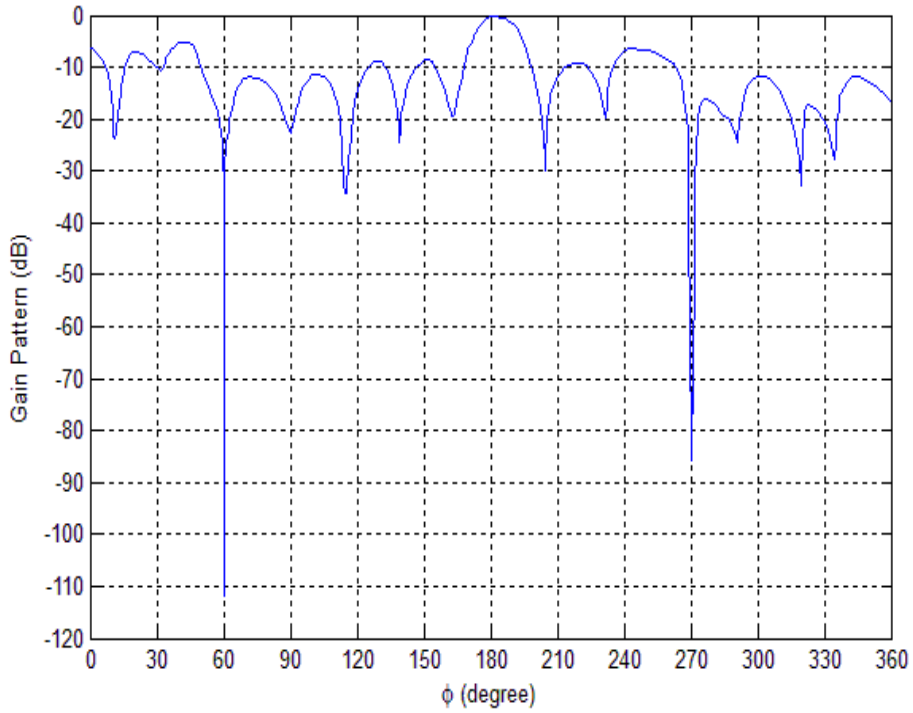


Figure 8. Normalized gain pattern for the hexagonal array

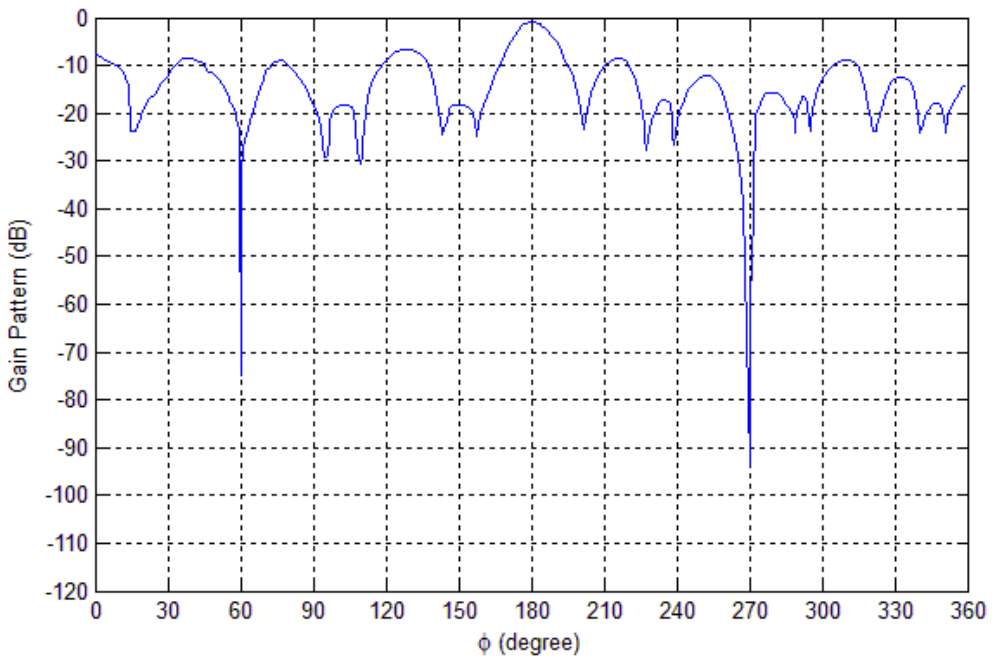


Figure 9. Normalized gain pattern for the octagonal array

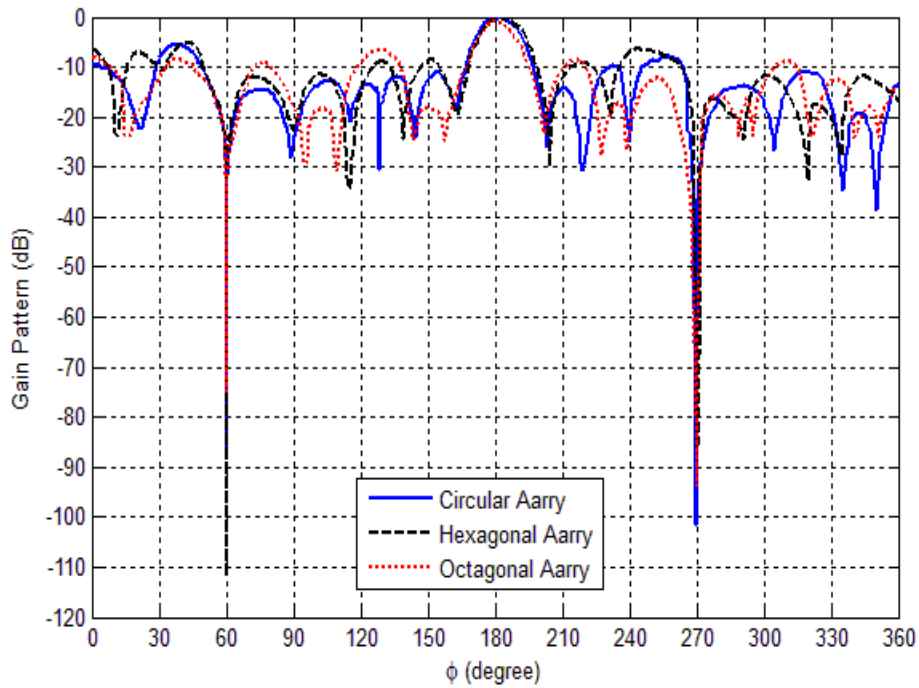


Figure 10. Comparison of the normalized gain pattern for Circular, Hexagonal and Octagonal arrays.

Table 1. Amplitude and phase excitation for each element and directivity comparison for different array types.

Element No.	Circular Arrays	Hexagonal Arrays	Octagonal Arrays
1	$3.00 \angle 74.5^\circ$	$2.65 \angle -142.8^\circ$	$1.66 \angle 162.7^\circ$
2	$2.98 \angle -90.3^\circ$	$3.00 \angle 78.4^\circ$	$2.03 \angle 35.8^\circ$
3	$2.99 \angle 54.2^\circ$	$3.00 \angle 55.9^\circ$	$2.54 \angle -122.6^\circ$
4	$1.69 \angle -81.7^\circ$	$3.00 \angle 156.3^\circ$	$1.62 \angle 19.5^\circ$
5	$2.44 \angle -17.43^\circ$	$3.00 \angle 114.8^\circ$	$3.00 \angle 118.3^\circ$
6	$2.91 \angle 170.1^\circ$	$3.00 \angle -39.2^\circ$	$3.00 \angle 132.7^\circ$
7	$3.00 \angle 180.0^\circ$	$1.62 \angle -94.5^\circ$	$3.00 \angle -81.6^\circ$
8	$3.00 \angle -67.5^\circ$	$2.09 \angle 22.6^\circ$	$3.00 \angle 78.1^\circ$
9	$3.00 \angle 45.2^\circ$	$1.17 \angle 167.2^\circ$	$3.00 \angle -8.6^\circ$

10	2.89 \angle 76.0 $^{\circ}$	2.34 \angle 144.3 $^{\circ}$	2.93 \angle -99.1 $^{\circ}$
11	2.97 \angle 132.6 $^{\circ}$	2.93 \angle 171.9 $^{\circ}$	1.72 \angle 64.3 $^{\circ}$
12	1.00 \angle 49.8 $^{\circ}$	2.91 \angle 81.6 $^{\circ}$	1.15 \angle 137.8 $^{\circ}$
13	2.15 \angle -10.7 $^{\circ}$	1.85 \angle 126.4 $^{\circ}$	2.33 \angle 45.2 $^{\circ}$
14	1.29 \angle -65.3 $^{\circ}$	1.24 \angle -5.7 $^{\circ}$	2.61 \angle 34.7 $^{\circ}$
15	3.00 \angle 161.2 $^{\circ}$	2.27 \angle 100.3 $^{\circ}$	2.98 \angle 12.6 $^{\circ}$
16	3.00 \angle 18.6 $^{\circ}$	2.92 \angle -14.9 $^{\circ}$	3.00 \angle -150.4 $^{\circ}$
17	2.83 \angle 180.0 $^{\circ}$	2.48 \angle -161.8 $^{\circ}$	1.84 \angle 143.9 $^{\circ}$
18	2.95 \angle 103.6 $^{\circ}$	3.00 \angle 177.4 $^{\circ}$	2.69 \angle 20.7 $^{\circ}$
19	1.36 \angle 83.4 $^{\circ}$	3.00 \angle 23.1 $^{\circ}$	1.25 \angle 71.2 $^{\circ}$
20	2.05 \angle 48.5 $^{\circ}$	2.13 \angle -129.3 $^{\circ}$	1.03 \angle -114.1 $^{\circ}$
21	1.96 \angle -30.7 $^{\circ}$	1.95 \angle 178.2 $^{\circ}$	2.77 \angle 109.5 $^{\circ}$
22	1.58 \angle 36.8 $^{\circ}$	1.36 \angle 44.9 $^{\circ}$	3.00 \angle 46.4 $^{\circ}$
23	3.00 \angle -26.2 $^{\circ}$	3.00 \angle -68.1 $^{\circ}$	2.92 \angle -57.0 $^{\circ}$
24	3.00 \angle 135.1 $^{\circ}$	1.17 \angle 56.3 $^{\circ}$	2.89 \angle 132.6 $^{\circ}$
Directivity	8.52 dB	6.63 dB	7.38 dB

5. CONCLUSION

In this paper, smart adaptive arrays such as Uniform circular arrays UCA, Uniform hexagonal arrays UHA and Uniform octagonal arrays UOA are considered. Each array consists of number of center-fed half-wave dipoles. The mutual coupling effects between the array elements are fully taken into account. By integrating the Central Force optimization (CFO) algorithm with the Hillclimbing (HC), the amplitudes and phases of the antennas are calculated for certain conditions. The comparison between circular, hexagonal, and octagonal array shows that hexagonal array geometry give slightly deeper nulls, a higher gain by approximately 1.89 dB and 0.75 dB, with respect to circular and Octagonal arrays. Moreover smaller overall size, with the same beamwidth as compared with these of the circular and octagonal array geometries.

6. ACKNOWLEDGEMENT

We would like to acknowledge the Electronics Research Institute (ERI), Microstrip Department, Giza, Cairo for the support, encouragement, help and cooperation during simulation process of this research.

7. REFERENCES

- [1] Chryssomallis, M., "Smart antennas," *IEEE Antennas and Propagation Magazine*, Vol. 42, No. 3, 129–136, June 2000.
- [2] Mouhamadou, M. and P. Vaudon, "Smart antenna array patterns synthesis: Null steering and multi-user beamforming by phase control," *Progress In Electromagnetics Research*, PIER 60, 95–106, 2006.
- [3] Ioannides, P. and C. A. Balanis, "Uniform circular arrays for smart antennas," *IEEE Antennas and Propagation Magazine*, Vol. 47, No. 4, 192–206, August 2005.
- [4] Ioannides, P. and C. A. Balanis, "Uniform circular and rectangular arrays for adaptive beamforming applications," *IEEE Antennas and Wireless Propagation Letters*, Vol. 4, 351–354, 2005.
- [5] Gozasht, F., G. R. Dadashzadeh, and S. Nikmehr, "A comprehensive performance study of circular and hexagonal array geometries in the LMS algorithm for smart antenna applications," *Progress In Electromagnetics Research*, PIER 68, 281–296, 2007.
- [6] Kretly, L. C., A. S. Cerqueira Jr., and A. A. S. Tavora, "A hexagonal adaptive antenna array concept for wireless communication applications," *The 13th IEEE International Symposium on Personal, Indoor and Mobile Radio Communications*, Vol. 1, 247–249, Sept. 15–18, 2002.
- [7] Haupt, R. L., "Phase-only adaptive nulling with a genetic algorithm," *IEEE Trans. on Antennas and Propagation*, Vol. 45, 1009–1015, 1997.
- [8] Varlamos, P. K. and C. N. Capsalis, "Electronic beam steering using switched parasitic smart antenna arrays," *Progress In Electromagnetics Research*, PIER 36, 101–119, 2002.
- [9] Gies, D. and Y. Rahmat-Samii, "Particle swarm optimization for reconfigurable phase-differentiated array design," *Microwave and Optical Technology Letters*, Vol. 38, No. 3, 168–175, August 2003.
- [10] Robinson, J. and Y. Rahmat-Samii, "Particle swarm optimization in electromagnetics," *IEEE Transactions on Antennas and Propagation*, Vol. 52, No. 2, 397–407, 2004.
- [11] Zainud-Deen, S. H., K. R. Mahmoud, M. El-Adawy, and S. M. M. Ibrahim, "Design of Yagi-Uda antenna and electromagnetically coupled curl antenna using particle swarm optimization algorithm," *TwentySecond National Radio Science Conference (NRSC 2005)*, Cairo, Egypt, March 15–17, 2005.
- [12] Chen, T. B., Y. B. Chen, Y. C. Jiao, and F. S. Zhang, "Synthesis of antenna array using particle swarm optimization," *Microwave Conference Proceedings, 2005. APMC 2005, Asia-Pacific Conference Proceedings*.
- [13] Donelli, M., R. Azaeo, F. G. B. Natale, and A. Massa, "An innovative computational approach based on a particle swarm strategy for adaptive phased-arrays control," *IEEE Transactions on Antennas and Propagation*, Vol. 54, No. 3, 888–898, March 2006.
- [14] Boeringer, D. W. and D. H. Werner, "Particle swarm optimization versus genetic algorithms for phased array synthesis," *IEEE Transactions on Antennas and Propagation*, Vol. 52, No. 3, 771–779, March 2004.

-
- [15] Khdir, M. M. and C. G. Christodoulou, "Linear array geometry synthesis with minimum sidelobe level and null control using particle swarm optimization," *IEEE Transactions on Antennas and Propagation*, Vol. 53, No. 8, 2674–2679, March 2005.
- [16] Bataineh, M. H. and J. I. Ababneh, "Synthesis of aperiodic linear phased antenna arrays using particle swarm optimization," *Electromagnetics*, Vol. 26, Issue 7, 531–541, October 2006.
- [17] Benedetti, M., R. Azaro, D. Franceschini, and A. Massa, "PSO-based real-time control of planar uniform circular arrays," *IEEE Antennas and Wireless Propagation Letters*, Vol. 5, 545–548, 2006.
- [18] Chen, T. B., Y. L. Dong, Y. C. Jiao, and F. S. Zhang, "Synthesis of circular antenna array using crossed particle swarm optimization algorithm," *J. of Electromagnetic Waves and Applications*, Vol. 20, No. 13, 1785–1795, 2006.
- [19] Su, T., K. R. Dandekar, and H. Ling, "Experimental study of mutual coupling compensation in smart antenna applications," *IEEE Trans. Antennas Propagat.*, Vol. AP-50, 480–486, 2002.
- [20] Gao, F., R.-H. Shan, and Q.-Z. Liu, "A novel circular smart antenna array implementation and its analysis with mutual coupling," *J. of Electromagnetic Waves and Appl.*, Vol. 18, No. 12, 1671–1678, 2004.
- [21] Huang, Z. Y., C. A. Balanis, and C. R. Birtcher, "Mutual coupling compensation in UCAs: Simulations and experiment," *IEEE Trans. on Antennas and Propagation*, Vol. 54, No. 11, pp. 3082–3086, November 2006.
- [22] Zainud-Deen, S. H., E. S. Mady, K. H. Awadalla, and H. A. Sharshar, "Adaptive arrays of smart antennas using genetic algorithm," *Twenty Second National Radio Science Conference (NRSC 2005)*, Arab Academy Science & Tech. and Maritime Transport, Cairo, Egypt, March 15–17, 2005.
- [23] Steyskal, H., R. A. Shore, and R. L. Haupt, "Methods for null control and their effects on the radiation pattern," *IEEE Transactions on Antennas and Propagation*, Vol. AP-34, No. 3, 404–409, March 1986.
- [24] K. R. Mahmoud, 'Central force optimization: Nelder-Mead hybrid Algorithm for Rectangular Microstrip Antenna Design,' *Electromagnetics*, Vol. 31, Issue 8, pp. 578-592, 2011.
- [25] Formato, R. A., "Central force optimization: A new metaheuristic with application in applied electromagnetics," *Progress in Electromagnetics Research PIER*, Vol. 77, pp.425-491, 2007.
- [26] Formato, R. A. 'Central force optimization: A new gradient-like metaheuristic for multidimensional search and optimization,' *Int. J. Bio-Inspired Computation*, Vol. 1, pp. 217-238, 2009.
- [27] Formato, R. A., 'Improved CFO algorithm for antenna optimization,' *Progress in Electromagnetics Research B*, Vol. 19, pp.405-425, 2010.
- [28] Qubati, G. M., R. A. Formato, and N. I. Dib., 'Antenna benchmark performance and array synthesis using central force optimization,' *IET Microwaves, Antennas & Propagation*, Vol. 4, pp.583-592, 2010.
- [29] K.R. Mahmoud, 'Design Optimization of a bow-tie antenna for 2.45GHz RFID readers using a hybrid BSO-NM algorithm,' *Progress In Electromagnetics Research*, PIER 100, pp. 105-117, 2010.

- [30] Andres Cano, Manuel Gomez, Serafin Moral," Application of a hill-climbing algorithm to exact and approximate inference in credal networks", 4th International Symposium on Imprecise Probabilities and Their Applications, Pittsburgh, Pennsylvania, 2005
- [31] A. M. Montaser, K. R. Mahmoud, and H. A. Elmikati, "An interaction study between pifas handset antenna and a human hand-head in personal communications," Progress In Electromagnetics Research B, Vol. 37, pp. 21-42, 2012.

تصميم أنظمة الهوائيات الذكية على شكل مصفوفات دائرية و سداسية و ثمانية باستخدام خوارزميات مركز القوى المهجنة

في هذا البحث تم عرض الخوارزميات الحديثة التي تسمى بمركز القوى وطرق التهجين بينها وبين الخوارزميات المحلية وتم تطبيقها على تصميم مصفوفة هوائيات ذكية في المحطة الاساسية ودراسة قدراتها على تشكيل الشعاع مع الاخذ في الاعتبار التأثير المتبادل وتم حساب تغذية المصفوفة على أن تكون أقرب ما يكون للمثالية ولكي نوضح كفاءة هذه الطريقة لتوجيه الاشارات في الاتجاه المطلوب وتقليلها في اتجاه الاشارات المتداخلة بواسطة التحكم في التغذية المركبة لكل عنصر في المصفوفة، هناك ثلاث أنواع من المصفوفات تم أخذهما في الاعتبار: مصفوفة دائرية منتظمة و سداسية منتظمة وثمانية منتظمة بغرض التقليل من المساحة المطلوبة للمصفوفة وتقليل مستوى الفص الجانبي. ولقد وجد أن الشكل الهندسي للمصفوفة السداسية تعطي عمق أضمحلالى أكبر في اتجاه الاشارات الغير مرغوب فيها وكسب أكبر ومستوى فص جانبي أقل ومساحة أصغر وذلك بنفس عرض الشعاع كما في أشكال المصفوفة الدائرية والثمانية.